

000 001 002 003 004 005 006 007 008 009 010 011 012 013 014 015 016 017 018 019 020 021 022 023 024 025 026 027 028 029 030 031 032 033 034 035 036 037 038 039 040 041 042 043 044 045 046 047 048 049 050 051 052 053 TRACEDET: HALLUCINATION DETECTION FROM THE DECODING TRACE OF DIFFUSION LARGE LANGUAGE MODELS

Anonymous authors

Paper under double-blind review

ABSTRACT

Diffusion large language models (D-LLMs) have recently emerged as a promising alternative to auto-regressive LLMs (AR-LLMs). However, the hallucination problem in D-LLMs remains underexplored, limiting their reliability in real-world applications. Existing hallucination detection methods are designed for AR-LLMs and rely on signals from *single-step* generation, making them ill-suited for D-LLMs where hallucination signals often emerge throughout the *multi-step* denoising process. To bridge this gap, we propose **TraceDet**, a novel framework that explicitly leverages the intermediate denoising steps of D-LLMs for hallucination detection. TraceDet models the denoising process as an *action trace*, with each action defined as the model’s prediction over the cleaned response, conditioned on the previous intermediate output. By identifying the sub-trace that is maximally informative to the hallucinated responses, TraceDet leverages the key hallucination signals in the multi-step denoising process of D-LLMs for hallucination detection. Extensive experiments on various open source D-LLMs demonstrate that **TraceDet** consistently improves hallucination detection, achieving an average gain in AUROC of **15.2%** compared to baselines.

1 INTRODUCTION

The auto-regressive large language models (AR-LLMs) (Achiam et al., 2023; Vaswani et al., 2017) have demonstrated unprecedented capabilities in content generation (Maleki & Zhao, 2024) and general task completion (Yao et al., 2023). Despite their success, AR-LLMs still face challenges related to generation efficiency and the reversal curse due to the inherent limitation of the next-token prediction paradigm (Bachmann & Nagarajan, 2024). The diffusion large language models (D-LLMs) have emerged as a promising alternative to AR-LLMs. Unlike AR-LLMs that generate language sequences from left to right, D-LLMs iteratively denoise the whole language sequences with a bi-directional attention architecture. Thus, D-LLMs have great potential in efficient computation and more flexible reasoning. Recent open-sourced works, such as LLaDA and Dream model series (Nie et al., 2025; Ye et al., 2025), have successfully scaled D-LLMs to 8B parameters, achieving performance comparable to leading AR-LLMs (AI, 2024) at the same scale in various tasks.

Although most work focuses on enhancing the capability of D-LLMs (Zhao et al., 2025; Yang et al., 2025b), less focus is devoted to their hallucination problem. Hallucination refers to generating linguistically plausible yet factually incorrect contents, which is recognized as a byproduct of the increasing capability of language models (Manakul et al., 2023; Zhang et al., 2025). The hallucination issue in D-LLMs undermines user trust and potentially causes severe consequences in critical domains (Huang et al., 2025), hindering their deployment in safety-critical scenarios.

Existing literature has focused on hallucination detection in AR-LLMs, which can be broadly categorized into output-based detection (Kossen et al., 2024) and latent-based detection (Du et al., 2024). Output-based detection leverages hallucination-related signals derived from model outputs, such as the consistency across multiple sampled responses (Kuhn et al., 2023) or the entropy of token-level logits. The intuition is that hallucinated responses are typically associated with lower confidence

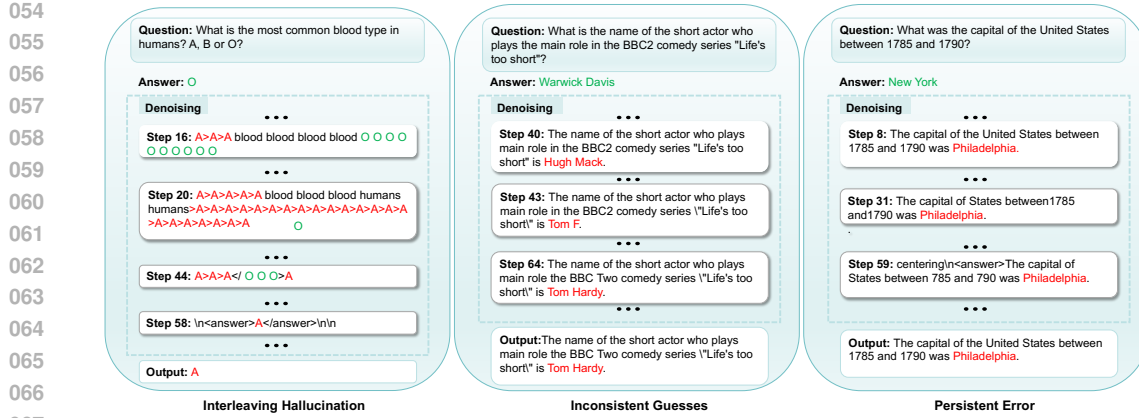


Figure 1: Illustration of representative D-LLM hallucination patterns extracted by TraceDet. Left: **Interleaving Hallucination**, where the model decodes both truthful and hallucinated content. Middle: **Inconsistent Guesses**, where multiple contradictory keywords lead to hallucination. Right: **Persistent Error**, where the model maintains a hallucinated answer throughout denoising. Hallucinations are highlighted with red.

(Rawte et al., 2023). Latent-based methods instead probe the hidden representations of AR-LLMs during a single forward pass to distinguish hallucinated from factual responses (Park et al., 2025; Li et al., 2025). Recent works further introduce new techniques to enhance the separation between hallucinated and factual responses in the latent space (Liu et al., 2025b; Orgad et al., 2025).

However, existing hallucination detection methods face challenges in detecting hallucinations in D-LLMs, since they typically exploit hallucination signals in the *single-step* generation process of AR-LLMs. Unlike AR-LLMs that produce responses in a single forward pass, D-LLMs iteratively refine the responses through a *multi-step* denoising process (Sahoo et al., 2024; Shi et al., 2024). Our empirical observations show that the hallucinated responses in D-LLMs are associated with an intriguing denoising process. As shown in Figure 1, some of them oscillate between factual and hallucinated content or randomly guess among various hallucinated answers, whereas others persistently maintain a single hallucinated answer throughout the denoising trajectory. While the underlying mechanism behind these behaviors remains an open question, these intermediate dynamics provide valuable signals for hallucination detection in D-LLMs.

Proposed work. We introduce **TraceDet**, a novel framework that leverages the intermediate denoising steps of D-LLMs for hallucination detection. The key insight is to represent the denoising process as an *action trace* (Black et al., 2024), where each action corresponds to the model’s prediction of a complete response sequence given the intermediate result at one denoising step. Rather than relying on the final output, TraceDet aims to identify a sub-trace of the whole action trace that contributes to the hallucinated responses (Section 3.2). The major difficulty is that the sub-trace of actions is not known *a priori*, leading to the absence of explicit action labels for supervision. Inspired by the information-bottleneck (IB) principle (Tishby et al., 2000), TraceDet identifies the sub-trace of actions that are maximally informative to the hallucinated response (Section 3.3). This informative sub-trace is then used to train a classifier for final hallucination detection (Section 3.4).

We extensively evaluate the capability of the proposed TraceDet on the two available open-source D-LLMs, including LLaDA-8B-Instruct and Dream-7B-Instruct, across three QA datasets covering multiple-choice, open-ended, and contextual answering tasks. On average, TraceDet delivers a consistent improvement of **15.2%** in hallucination detection accuracy (AUROC), and further studies also confirm the robustness of the proposed method to varying denoising strategies and hyperparameter settings. Our main contributions are threefold:

- We make an initial effort in the study of hallucination behaviors in D-LLMs, uncovering distinctive multi-step patterns, such as interleaving hallucination, inconsistent guesses, and persistent errors, that are absent in AR-LLMs.
- We introduce **TraceDet**, a novel hallucination detection framework that formulates the D-LLM denoising process as an action trace. By applying the information bottleneck prin-

108
109
110
111
112
113
114
115
116
117
118
119
120
121
122
123
124
125
126
127
128
129
130
131
132
133
134
135
136
137
138
139
140
141
142
143
144
145
146
147
148
149
150
151
152
153
154
155
156
157
158
159
160
161
ciple, TraceDet automatically extracts the most informative sub-trace for detection, without
requiring explicit step-level supervision.

- We conduct comprehensive experiments on two open-source D-LLMs (LLaDA-8B-Instruct, Dream-7B-Instruct) across diverse QA benchmarks, where our method shows an average AUROC improvement of 15.2% over the baselines and demonstrates robustness across different denoising strategies and hyperparameter choices.

2 RELATED WORK

Hallucination Detection is a central problem in ensuring the safety, truthfulness, and faithfulness of LLM-based applications (Huang et al., 2025). Existing works have mainly been developed for AR-LLMs, and can be categorized as: (a) *Output-based*: calculating measures based on output signals such as semantic entropy (Kuhn et al., 2023), lexical similarity (Lin et al., 2023) and so on (Ren et al., 2022; Malinin & Gales, 2020; Xiong et al., 2023; Lin et al., 2022; Kuhn et al., 2023; Manakul et al., 2023); (b) *Latent-based*: probing hidden states from one-pass generations (Azaria & Mitchell, 2023; Chen et al., 2024a; Du et al., 2024; Su et al., 2024; Chen et al., 2024b; Li et al., 2023; Kossen et al., 2024; Marks & Tegmark, 2023; Kim et al., 2024; Chen et al., 2024a). While effective in AR-LLMs, existing methods face challenges in D-LLMs due to mismatches between final outputs and the intermediate denoising process, as well as the restricted availability of output token logits. We discuss the most relevant literature with our work, and defer the details to Appendix B.

Diffusion Large Language Model extends the success of diffusion models (Yang et al., 2023; Lu et al., 2025) to texts (Li et al., 2022). Nie et al. (2025) adopts an alternative discrete feature unifying the discrete remasking process, and has successfully scaled the D-LLM up to an 8B parameter level, achieving performance comparable to leading LLMs such as LLaMA-3 (AI, 2024). In addition, Dream-7B (Ye et al., 2025) adopts the same configurations as Qwen2.5-7B (Yang et al., 2025a) trained under a diffusion paradigm. Despite these advances, the hallucination problem in D-LLMs remains underexplored, hindering their application in real-world scenarios.

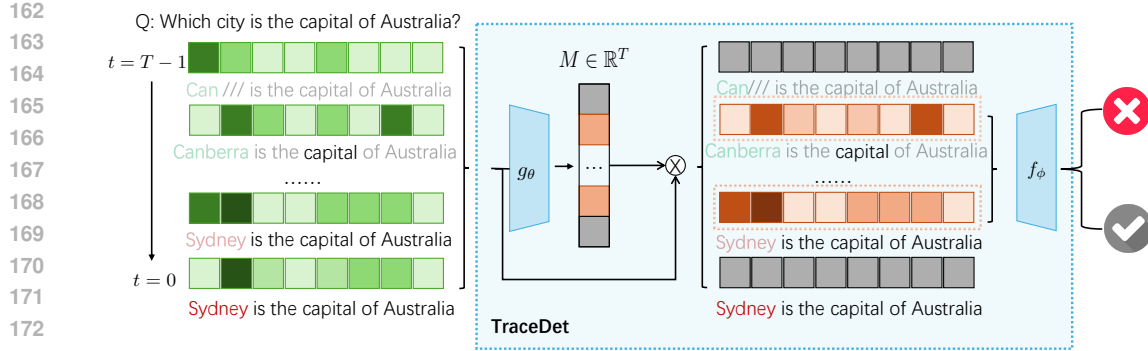
Information Bottleneck principle was initially proposed in signal processing to extract the most informative sub-instances while minimizing irrelevant information, and has gained lots of applications in deep learning (Alemi et al., 2016; West et al., 2019; Zhu et al., 2024; Luo et al., 2019). However, its use in hallucination detection remains largely unexplored due to the limited information available in a single text generation. The most related work (Bai et al., 2025) integrates IB into VLLM as a sub-instance extractor for images, mitigating hallucination in VLLM outputs. Our work builds on the sequential and information-excess nature of stepwise D-LLM generations. We propose a temporal embedding approach that captures intermediate step signals to detect hallucinations.

3 HALLUCINATION DETECTION IN DIFFUSION LLMs

3.1 PROBLEM FORMULATION

Unlike AR-LLMs, D-LLMs generate responses by iterative refinement through a forward noising and backward denoising process over T time steps. Let $r = (r_0, \dots, r_T)$ denote the sequence of intermediate texts, where each $r_t \in \mathbf{V}^n$ is a token sequence of length n and $r_t^i \in \mathbf{V}$ for $i \in \{1, \dots, n\}$. Here, r_0 is the clean text sequence and r_T the fully masked sequence, with $t \in \{0, \dots, T\}$. Given a prompt p_0 , the forward noising process is defined by a sequence of distributions $\{q(r_t | r_{t-1})\}_{t=1}^T$, and can be written as $q(r_{1:T} | r_0) = \prod_{t=1}^T q(r_t | r_{t-1})$.

The reverse denoising process with discrete remasking is parameterized by the sequence of conditional distributions $\{P_\theta(r_0 | r_t, p_0)\}_{t=1}^T$. At each timestep $t > 0$, the model predicts all masked tokens from r_t : $\tilde{r}_{t-1} \sim P_\theta(r_0 | r_t, p_0)$, and then a fraction ρ_t of tokens in r_t are remasked to form r_{t-1} . As proposed in Nie et al. (2025), current popular remasking strategies often use low-confidence remasking, which retains the highest confidence tokens during each remasking step. After T iterations, the process outputs the final response r_0 .



Given an input query p_0 , the hallucination detection can be formulated as binary classification:

$$\min_{h \in \mathcal{H}} \mathcal{L}(Y, h(r_0)), \quad s.t. \quad r_0 \sim \prod_{t=T-1}^0 P_\theta(r_t | r_{t+1}, p_0), \quad (1)$$

where r_0 is the final response from the D-LLM, which can be either a hallucinated or non-hallucinated (or factual) answer, where $Y \in \{0, 1\}$ is the ground-truth label indicating if r_0 is a hallucinated answer, h is the classifier belonging to some hypothesis space \mathcal{H} and $\mathcal{L}(\cdot)$ is the cross-entropy loss, and r_{T-i} is the intermediate sequence produced at the i -th denoising step. Since hallucination detection directly on generated text is costly and difficult to implement in practice, we instead rely on auxiliary signals derived from the generation process.

3.2 OVERVIEW OF TRACEDET

Denoising as a Markov Decision Process. The major challenge of hallucination detection in D-LLMs is the mismatch between the intermediate model generation and the final response. More specifically, it is challenging to determine how hallucination arises in the final response and utilize this information for detection, as partial information in the generated sequence can be erased during multi-step denoising and remasking. Essentially, the denoising process of D-LLMs can be formulated as a Markov Decision Process (MDP) over decoding steps (Black et al., 2024):

- **State:** We define the t -th state $s_t = (p_0, r_{T-t})$ in the denoising process as the combination of the input query p_0 and the intermediate sequence r_{T-t} at the t -th denoising step.
- **Action:** At the t -th state, the D-LLM predicts all masked tokens from s_t and generates a full token sequence \tilde{r}_{T-t-1} from distribution $P_\theta(r_0 | r_{T-t}, p_0)$.
- **Transition:** After generating \tilde{r}_{T-t-1} , a fraction of tokens is remasked to form r_{T-t-1} depending on the noise schedule and remasking strategy. Then, the D-LLM moves to the next state $s_{t+1} = (p_0, r_{T-t-1})$ to start another round of denoising.

Hallucination Detection from Action Trace. With the MDP formulation, we can leverage the entire action trace $A = \{a_0, a_1, \dots, a_{T-1}\}$ rather than only the final response r_0 to detect hallucinations. Each action reveals how the model progressively refines its generation. Our observations in Figure 1 show that hallucinated outputs are strongly associated with intermediate denoising steps, especially when the intermediate outputs contain distracting or ambiguous content. Additional examples are provided in Appendix F. TraceDet exploits this insight by discovering hallucination-relevant action sub-trace A_{sub} from A , and then trains a classifier f on A_{sub} to distinguish hallucination from factual responses:

$$\min_{f,g} \mathcal{L}(Y, f(A_{sub})), \quad s.t. \quad A_{sub} = g(A). \quad (2)$$

216 Here $g(\cdot)$ is a neural network that identifies A_{sub} from A . By capturing hallucination signals
 217 throughout the entire action trace, TraceDet provides an interpretable and fine-grained perspective
 218 on how hallucinations emerge during the denoising trajectory. Moreover, TraceDet can be applied
 219 to diverse D-LLMs with different noise schedules and remasking strategies.
 220

221 3.3 OPTIMIZATION OF TRACEDET VIA INFORMATION-THEORETIC APPROACH

223 A key challenge of TraceDet lies in the fact that hallucination-relevant actions in the denoising
 224 trajectory of D-LLMs are not known *a priori*. The hallucination-relevant action may be sparse
 225 and unevenly distributed across the action trace, and not every action contributes equally to the
 226 emergence of hallucination. This necessitates learning to identify such a sub-trace A_{sub} from A
 227 that is informative to the hallucinated response, in the absence of explicitly labeled A_{sub} . Inspired
 228 by the information bottleneck principle (Tishby et al., 2000; Tishby & Zaslavsky, 2015), TraceDet
 229 reformulates the objective in Eq. 2 from an information-theoretic perspective:
 230

$$\min_{\substack{f: A_{sub} \rightarrow Y \\ g: A \rightarrow A_{sub}}} -I(Y; A_{sub}) + \beta I(A; A_{sub}), \quad (3)$$

232 where $I(A; B) = \iint_{A, B} P(A, B) \log \frac{P(A, B)}{P(A)P(B)} dA dB$ is the mutual information between the ran-
 233 dom variable A and B . The first term $I(Y; A_{sub})$ in Eq. 3 encourages the identified A_{sub} is relevant
 234 to the hallucination and the second term $I(A; A_{sub})$ regularizes the identified A_{sub} only contains
 235 partial information of A to avoid the trivial solution $A_{sub} = A$. β is the hyperparameter to trade off
 236 between the two terms. **By trading off between the two terms in Eq. 3, TraceDet aims to identify the**
 237 ***minimally sufficient* sub-trace in the denoising process of D-LLMs for hallucination detection.**
 238

239 Furthermore, as the mutual information related objectives are often intractable and hard to optimize,
 240 we need to resort more practical forms of Eq. 3. We begin by examining the first term in Eq. 3:

$$-I(Y; A_{sub}) \leq \mathbb{E}_{Y, A_{sub}} [-\log q_{\theta}(Y | A_{sub})] := \mathcal{L}_{cls}(f(A_{sub}), Y). \quad (4)$$

242 Here $q_{\theta}(Y | A_{sub})$ is the variational approximation to $p(Y | A_{sub})$, which corresponds to the classi-
 243 fier $f(\cdot)$ that predicts whether the identified sub-trace is relevant to the hallucination. And $\mathcal{L}_{cls}(\cdot)$ is
 244 the classification loss, and we choose the cross-entropy loss in practice. Then, we proceed to derive
 245 the upper bound of the second term $I(A; A_{sub})$ in Eq. 3:

$$\begin{aligned} I(A; A_{sub}) &= \mathbb{E}_{A, A_{sub}} \left[\log \frac{P(A_{sub} | A)}{Q(A_{sub})} \right] - D_{KL}(P(A_{sub}) \| Q(A_{sub})) \\ &\leq \mathbb{E}_A \left[D_{KL}(P(A_{sub} | A) \| Q(A_{sub})) \right], \end{aligned} \quad (5)$$

246 where $D_{KL}(\cdot \| \cdot)$ is the KL-divergence (Kullback & Leibler, 1951). The inequality in Eq. 5 is induced
 247 using the non-negative nature of the KL-divergence. Recall that $A = \{a_0, a_1, \dots, a_{T-1}\}$, the pos-
 248 terior distribution $P(A_{sub} | A)$ can be factorized into $\prod_{a_i \in A} \text{Bernoulli}(p_{a_i})$ where we assume that
 249 the sub-instance extractions of A are independent. The corresponding prior distribution $Q(A_{sub})$
 250 in Eq. 5 is the non-informative distribution $\prod_{a_i \in A} \text{Bernoulli}(\tau)$, where τ restricts the proportion
 251 of traces that will be selected. **To this end, we relax Eq. 5 and approximate it by the following**
 252 **differentiable objective as discussed in Appendix D:**

$$\mathcal{L}_{ext} = \sum_{i=0}^{T-1} \left[p_{a_i} \log \frac{p_{a_i}}{\tau} + (1 - p_{a_i}) \log \frac{1 - p_{a_i}}{1 - \tau} \right], \quad (6)$$

253 where p_{a_i} is the predicted probability to select trace a_i . For consistency and unification, we train the
 254 composed function $f \circ g(A)$ with the following learning objective:
 255

$$\mathcal{L} = \mathcal{L}_{cls} + \beta \mathcal{L}_{ext}, \quad (7)$$

256 where β is the same hyperparameter as in Eq. 3, controlling the strength of the regularization term.
 257

258 3.4 IMPLEMENTATION

259 For our method, we define the action trace using distributional statistics, specifically the token-wise
 260 entropy trace derived from P_{θ} . This choice captures the temporal evolution of uncertainty during

270 Table 1: AUROC(%) comparison of hallucination detection methods on two D-LLMs across three
 271 QA datasets with 128 and 64 generation step lengths. SS is the short for Single Sampling. The
 272 highest score is **bolded** and the second highest is underlined.

274 Model	275 Method	276 SS	277 TriviaQA		278 HotpotQA		279 CommonsenseQA		280 Ave
			128	64	128	64	128	64	
Output-Based									
281 LLaDA-8B-Instruct	Perplexity	X	50.4	47.6	49.3	51.2	65.6	65.0	54.9
	LN-Entropy	X	54.6	<u>53.5</u>	54.8	54.7	<u>64.6</u>	<u>64.4</u>	57.8
	Semantic Entropy	X	68.9	<u>67.3</u>	57.6	53.8	44.1	43.9	55.9
	Lexical Similarity	X	62.5	<u>59.0</u>	64.2	57.1	57.3	60.7	60.1
Latent-Based									
282 EigenScore	EigenScore	X	<u>69.2</u>	66.9	64.7	59.2	58.5	60.6	<u>63.2</u>
	CCS	✓	<u>57.1</u>	54.2	57.6	55.8	50.5	58.5	<u>55.6</u>
	TSV	✓	60.2	61.1	<u>65.0</u>	<u>59.4</u>	52.9	55.2	59.0
	TraceDet	✓	73.9	74.1	66.1	63.7	77.2	77.1	72.0
Output-Based									
285 Dream-7B-Instruct	Perplexity	X	-	-	-	-	-	-	-
	LN-Entropy	X	-	-	-	-	-	-	-
	Semantic Entropy	X	73.7	72.5	<u>62.7</u>	<u>67.7</u>	51.4	48.6	62.8
	Lexical Similarity	X	58.3	64.0	59.7	62.7	<u>77.3</u>	76.9	66.5
Latent-Based									
290 EigenScore	EigenScore	X	66.0	69.1	62.5	67.0	76.9	<u>77.5</u>	<u>69.8</u>
	CCS	✓	56.9	50.3	51.7	58.2	54.2	53.2	<u>54.1</u>
	TSV	✓	<u>75.6</u>	<u>74.7</u>	58.7	63.0	62.3	56.8	65.2
	TraceDet	✓	78.1	86.7	75.1	76.0	84.7	84.1	80.8

294 generation while yielding a fixed-size representation. Alternatively, one could construct action traces
 295 from the token embeddings of \tilde{r} . However, embedding-based traces, particularly when combined
 296 with temporal encodings, make the representation extremely large and often introduce severe numerical
 297 instabilities in practice. **Our detection model is decomposed into two learnable modules: the**
 298 **sub-instance extractor g_θ and the sub-instance predictor f_ϕ , with implementation and complexity**
 299 **details discussed in Appendix H:**

301 (a) **Sub-instance extractor:** Given the entropy sequence $A \in \mathbb{R}^{T \times B \times D}$, we concatenate it with
 302 sinusoidal time embeddings and encode the result using a Transformer (Queen et al., 2023; Liu
 303 et al., 2024), yielding contextual embeddings emb . The extractor then produces a probabilistic
 304 mask $\hat{M} \in (0, 1)^{T \times B}$, where $\hat{m}_{t,b} = \text{Linear}(\text{attn}(emb, A))$, with attn a cross-attention
 305 mechanism using emb as query and a representation of A as key/value. A temporal binary mask
 306 $M \in \{0, 1\}^{T \times B}$ is then sampled from \hat{M} and applied to A , i.e., $A_{\text{sub}} = M \odot A \in \mathbb{R}^{T \times B \times D}$,
 307 where \odot denotes element-wise multiplication. However, the mask sampling process is inherently
 308 non-differentiable, so we employ the Gumbel–Softmax trick (Jang et al., 2016).

309 (b) **Sub-instance predictor:** The masked trajectory A_{sub} is temporally aggregated and passed to the
 310 predictor f_ϕ , which directly outputs hallucination probabilities $f_\phi(A_{\text{sub}}) \in [0, 1]$, $b = 1, \dots, B$.
 311 In practice, f_ϕ consists of temporal aggregation followed by an MLP and an activation layer.

313 4 EXPERIMENTS

315 4.1 SETUP

317 **Datasets.** We conduct experiments on three widely used factuality QA benchmarks: **TriviaQA**
 318 (Joshi et al., 2017) consists of open-domain factoid questions with answer spans in Wikipedia.
 319 **CommonsenseQA** (Talmor et al., 2018) contains multiple-choice questions requiring commonsense
 320 reasoning. **HotpotQA** (Yang et al., 2018) contains multi-hop questions requiring aggregation across
 321 supporting contexts. These datasets enable the evaluation of hallucination detection across varying
 322 reasoning complexity. For each dataset, we randomly sample 400 QA pairs from the validation split
 323 with available ground-truth labels, partitioned into 200 validation and 200 testing instances to ensure
 324 computational efficiency while maintaining task coverage.

324
325
326
327 Table 2: **F1 score (%)** comparison between TraceDet and baseline methods. The highest score is
328 **bolded**.
329
330
331
332
333

Method	TriviaQA		HotpotQA		CommonsenseQA	
	128	64	128	64	128	64
Lexical Similarity	49.9	50.6	59.8	55.2	80.0	82.6
EigenScore	56.0	51.8	63.9	56.9	79.8	82.9
CCS	59.3	65.0	47.3	53.0	61.0	53.5
TSV	70.5	67.6	68.5	65.1	62.5	57.6
TraceDet	76.7	<u>80.2</u>	73.8	68.7	89.7	90.2

334
335 Table 3: AUROC(%) comparison between TraceDet and our proposed baselines (Ave Entropy,
336 TraceDet w/o Masking). The highest score is **bolded** and the second highest is underlined.
337
338
339
340
341
342
343

Model	Method	TriviaQA		HotpotQA		CommonsenseQA		Ave
		128	64	128	64	128	64	
LLaDA-8B-Instruct	Ave Entropy	61.3	68.3	56.2	58.1	63.8	68.8	62.8
	TraceDet w/o Masking	<u>71.2</u>	<u>70.3</u>	<u>63.2</u>	<u>61.6</u>	<u>73.1</u>	<u>75.2</u>	<u>69.1</u>
	TraceDet	73.9	74.1	66.1	63.7	77.2	77.1	72.0
Dream-7B-Instruct	Ave Entropy	59.1	69.9	50.8	57.8	77.1	76.9	65.3
	TraceDet w/o Masking	<u>76.2</u>	87.1	<u>72.5</u>	<u>74.1</u>	<u>81.4</u>	<u>79.1</u>	<u>78.4</u>
	TraceDet	78.1	<u>86.7</u>	75.1	76.0	84.7	84.1	80.8

344
345
346 **Baseline Methods.** We compare our method against seven baselines spanning two categories pro-
347 posed in Section 2: (1) Output-based methods: **Perplexity** (Ren et al., 2022), Length-Normalized
348 Entropy (**LN-Entropy**) (Malinin & Gales, 2020), **Semantic Entropy** (Kuhn et al., 2023), and **Lex-
349 ical Similarity** (Lin et al., 2023); (2) Latent-based methods: **EigenScore** (Chen et al., 2024a),
350 Contrast-Consistent Search (CCS) (Burns et al., 2022), and Truthfulness Separator Vector (**TSV**)
351 (Park et al., 2025). We also include two TraceDet variants. **Ave Entropy** uses the average of step-
352 wise entropies as a naive confidence measure. In **TraceDet w/o Masking**, we train a transformer
353 detector while removing the sub-step extraction and its associated loss. All methods use identical
354 dataset splits, random seeds, and configurations to ensure fair comparison.355
356 **Models.** We adopt **Dream-7B-Instruct** (Ye et al., 2025) and **LLaDA-8B-Instruct** (Nie et al., 2025)
357 as representative D-LLMs in this work. To the best of our knowledge, they are the only open-
358 source D-LLMs that provide stepwise token-level logits and hidden representations necessary for
comprehensive baseline comparison across both Output-based and Latent-based detection methods.359
360 **Evaluation.** We employ task-specific evaluation protocols: multiple-choice tasks are evaluated by
361 direct comparison with the ground-truth, while Qwen3-8B (Yang et al., 2025a) serves as an external
362 judge for hallucination assessment in open-domain QA. We further measured the agreement between
363 the Qwen3-8B judge and human evaluation, finding 90% consistency on TriviaQA and 84% on
364 HotpotQA. Following previous work (Park et al., 2025; Chen et al., 2024a), we report AUROC
365 scores, with model selection based on validation performance and evaluation on held-out test sets.366
367

4.2 MAIN RESULTS

368
369 Table 1 presents a comprehensive comparison of TraceDet against baseline hallucination detec-
370 tion methods across two D-LLMs and three factuality QA datasets with varying generation lengths.
371 TraceDet achieves the highest performance in all experimental settings, outperforming the second
372 strongest baseline by 8.8% AUROC on LLaDA-8B-Instruct and 11% on Dream-7B-Instruct. These
373 consistent gains exhibit the value of exploiting temporal denoising dynamics rather than relying
374 solely on output uncertainty or static hidden-state representations. Among the baselines, Output-
375 based approaches suffer from poor consistency, with LN-Entropy and Perplexity methods showing
376 high variance across datasets on the LLaDA-8B-Instruct model. Due to restricted access to inter-
377 mediate logits from Dream-7B-Instruct, our attempts to estimate Perplexity and LN-Entropy suffer
378 from severe numerical instabilities, often diverging to infinity. Moreover, Semantic Entropy achieves
379 75.1% AUROC on TriviaQA with Dream-7B-Instruct but collapses to 51.4% on CommonsenseQA,
380 underscoring poor robustness when hallucinations decouple from token-level ambiguity. Latent-

378

Table 4: Average inference time of 100 samples for different methods.

379

380

381

382

383

384

385

386

387

388

389

390

391

392

393

394

395

396

397

398

399

400

401

402

403

404

405

406

407

408

409

410

411

412

413

414

415

416

417

418

419

420

421

422

423

424

425

426

427

428

429

430

431

Metric	Perplexity	LN-Entropy	Semantic Entropy	Lexical Similarity	EigenScore	CCS	TSV	TraceDet
Time (s) ↓	468.44	710.63	801.35	715.35	693.46	140.73	160.31	147.52

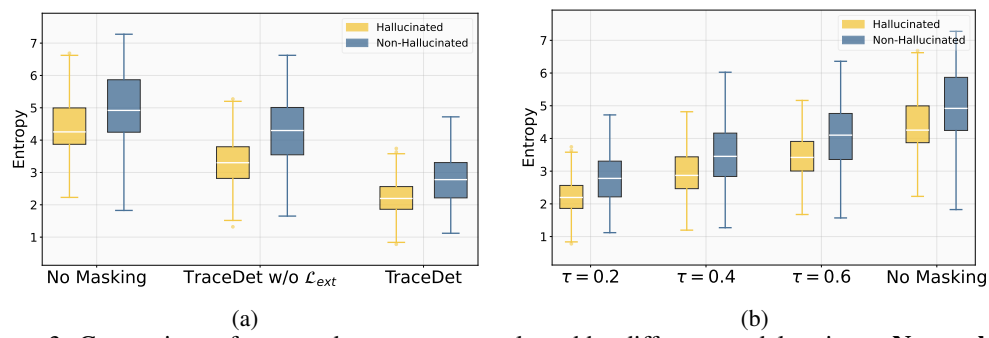


Figure 3: Comparison of averaged trace entropy selected by different model variants. **No masking** refers to the full time step traces. (a) Comparison between different model variants. (b) Comparison between different masking ratios τ . Results are reported using Dream-7B-Instruct.

based methods capture hidden-state geometry and show more competitive results, but they remain sensitive to dataset and model choice. TSV achieves 75.6% AUROC on TriviaQA with Dream-7B-Instruct yet fluctuates significantly across tasks while consistently underperforming TraceDet. **This superiority is not limited to AUROC, TraceDet also achieves the highest F1 scores across all dataset–model combinations, further confirming its robustness illustrated in Table 2.**

To isolate the contributions of our training framework and the IB principle, we evaluate two ablations in Table 3: Ave Entropy and TraceDet w/o Masking. Naively averaging stepwise entropy yields insufficient performance, while training without masking improves results but still underperforms TraceDet. This demonstrates that the IB principle enables TraceDet to identify maximally informative sub-instances, yielding clear improvements over both simplified variants.

4.3 ANALYSIS

Understanding TraceDet. The core idea of TraceDet is to select a sub-trace A_{sub} that preserves steps predictive of hallucination. To analyze the statistical properties of the extracted sub-traces, we utilize the stepwise maximum token entropy H_t^{\max} , and summarize each example by the mean over the selected steps $\bar{E} = \frac{1}{|S|} \sum_{t \in S} H_t^{\max}$. We compare three variants: (i) No Masking, which uses the full trajectory ($A_{sub} = A$); (ii) TraceDet w/o \mathcal{L}_{ext} , the same architecture trained without the extraction loss; and (iii) TraceDet. Figure 3a shows that TraceDet reduces both the mean and variance of \bar{E} while preserving separation between hallucinated and non-hallucinated examples, indicating that masking serves as an effective regularization mechanism. It reduces the maximum entropy among the selected steps, removing noisy or unstable transitions, while still preserving the entropy contrast that distinguishes hallucinated from non-hallucinated examples. Removing masking weakens this effect. Varying the masking ratio τ (Fig. 3b) confirms that stronger masking more aggressively removes steps with maximum token entropy without reducing the discriminative separation required for reliable detection.

Efficiency. TraceDet is highly efficient at inference. Unlike AR-LLMs, D-LLMs generate text through iterative denoising, where each forward pass is computationally more costly. This makes inference efficiency especially important for hallucination detection in D-LLMs. Existing methods impose significant computational overhead through two types of multi-sample computations: (i) Monte-Carlo sampling over output log-likelihood for estimating Perplexity or LN-Entropy, requiring typically at least 128 remasking samples for stable results (Nie et al., 2025), and (ii) response sampling for similarity-based metrics like Lexical Similarity or Semantic Entropy, multiplying inference cost by the number of samples S . TraceDet eliminates this overhead by directly leveraging stepwise entropy signals naturally exposed during denoising, requiring no additional sampling. Table 4

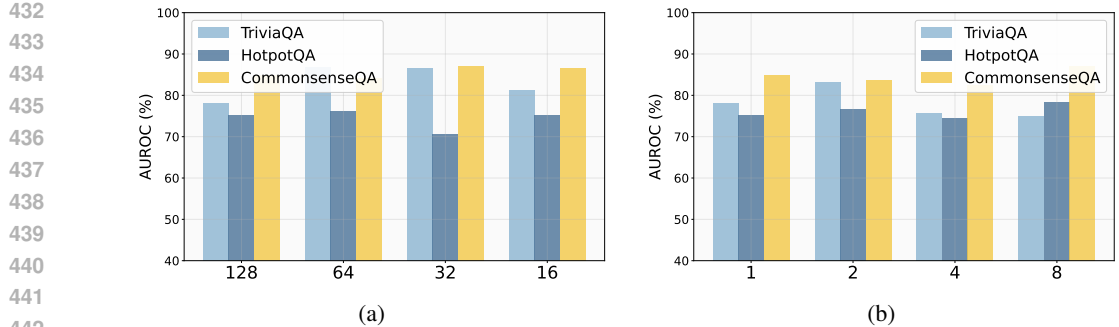


Figure 4: (a) TraceDet performance of different generation lengths with step length fixed at 1. (b) TraceDet performance with different step lengths with generation length fixed at 128. All results are reported as AUROC using Dream-7B-Instruct.

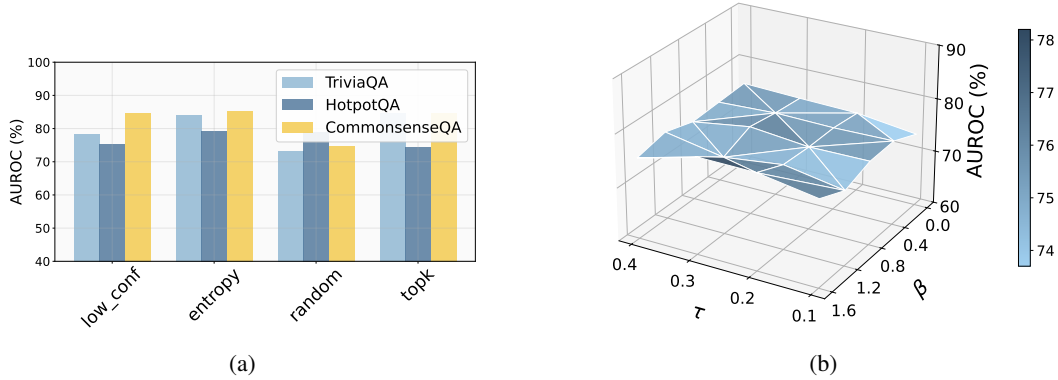


Figure 5: (a) TraceDet performance sensitivity to remasking strategies. (b) TraceDet performance sensitivity to \mathcal{L}_{ext} parameters τ and β on TriviaQA. All results are reported as AUROC using Dream-7B-Instruct.

demonstrates that TraceDet achieves better performance while significantly reducing inference cost compared to multi-sampling baselines. All timing results are reported on the LLaDA-8B-Instruct model on the same hardware device with S set to 10, which aligns with practical application settings.

Sensitivity to Generation Length and Step Length. D-LLMs typically generate sequences with fixed lengths, making parameter sensitivity analysis crucial for practical deployment. Generation length determines the entropy matrix dimensionality, while step length controls token retention at each denoising step. To assess the influence of these parameters, we conduct sensitivity analysis by varying generation length $L \in \{16, 32, 64, 128\}$ with step length fixed at 1 (Figure 4a), and step length $S \in \{1, 2, 4, 8\}$ with generation length fixed at 128 (Figure 4b).

TraceDet demonstrates robust performance across parameter ranges. As shown in Figure 4a, TraceDet achieves optimal performance at moderate lengths (64 and 32 tokens), with slight deterioration at the longest setting (128 tokens). This suggests that excessively long sequences may introduce noise that dilutes the hallucination signal. For fact-based QA tasks like TriviaQA, where answers are typically concise, generation length 64 provides sufficient reasoning capacity while maintaining detection quality. Figure 4b shows that step length has minimal impact on performance, with all settings yielding comparable results across datasets. The consistent performance across both parameter dimensions indicates that TraceDet’s effectiveness is not critically dependent on generation settings, making it practically robust for deployment across diverse D-LLM configurations.

Sensitivity to Remasking Strategies. Figure 5a examines the impact of different remasking strategies on TraceDet’s performance with Dream-7B-Instruct across four approaches: low-confidence (retaining most confident predictions), entropy (retaining lowest entropy tokens), random (random retention), and top-k (retaining based on top-1/top-2 confidence margins). TraceDet maintains robust performance across most strategies, with AUROC scores ranging from 75-85% on TriviaQA

486 and CommonsenseQA. However, random remasking shows degraded performance on TriviaQA,
 487 likely because random token retention disrupts the model’s ability to maintain coherent reasoning
 488 patterns essential for fact-based question answering. The stability across remasking strategies (low-
 489 confidence, entropy, top-k) demonstrates TraceDet’s adaptability to different D-LLM configurations.
 490

491 **Sensitivity to Hyperparameters.** Figure 5b analyzes the sensitivity of TraceDet to the \mathcal{L}_{ext} hy-
 492 perameters τ (masking ratio) and β (regularization weight). The 3D surface plot reveals a stable
 493 performance plateau across a wide range of parameter combinations. TraceDet achieves optimal
 494 performance when $\tau \in [0.2, 0.3]$ and $\beta \in [0.8, 1.6]$, indicating that retaining 20-30% of denois-
 495 ing steps with moderate regularization provides the best balance between information preserva-
 496 tion and noise reduction. The broad stability region demonstrates that TraceDet does not require precise
 497 hyperparameter tuning for effective deployment.
 498

5 CONCLUSION

500 In this work, we addressed the challenge of hallucination detection in D-LLMs by introducing a new
 501 framework, **Decoding Trace Detection (TraceDet)**. TraceDet is a lightweight, diffusion model ar-
 502 chitecture-aware detector built upon information bottleneck principles, which identifies sufficient
 503 sub-instances from the denoising entropy matrix. Our experiments demonstrate that **TraceDet** con-
 504 sistently achieves superior performance on mainstream D-LLMs across multiple datasets. Beyond
 505 proposing a new hallucination detection method, this work also offers insights into the mechanisms
 506 of hallucination generation in D-LLMs, paving the way toward building more reliable applications
 507 of D-LLMs. As future work, we will focus on developing strategies to mitigate the proposed hal-
 508 lucinated patterns. We believe the insights from TRACEDET can inspire future methods that more
 509 effectively leverage decoding traces as reliable supervision signals for improved detection.
 510
 511
 512
 513
 514
 515
 516
 517
 518
 519
 520
 521
 522
 523
 524
 525
 526
 527
 528
 529
 530
 531
 532
 533
 534
 535
 536
 537
 538
 539

540 ETHICS STATEMENT
541

542 This research did not involve identifiable human data or animals and therefore did not require ap-
543 proval from an institutional ethics committee or review board. All experiments are conducted on
544 publicly available datasets for scientific purposes only. The work does not involve or target any sen-
545 sitive attributes such as gender, race, nationality, or skin color. Our study focuses on hallucination
546 detection in diffusion large language models, with the aim of improving the reliability and safety of
547 LLMs.

548
549 REPRODUCIBILITY STATEMENT
550

551 We have made every effort to ensure the reproducibility of our work. All experiments were con-
552 ducted using publicly available datasets, and we provide detailed descriptions of data preprocessing
553 in Section 4. Our model architecture, hyperparameters, and training protocols are fully specified in
554 Section 3 and Appendix E. We will release our code and scripts for data processing and evaluation
555 upon publication to facilitate replication.

556 REFERENCES
557

558 Josh Achiam, Steven Adler, Sandhini Agarwal, Lama Ahmad, Ilge Akkaya, Florencia Leoni Ale-
559 man, Diogo Almeida, Janko Altenschmidt, Sam Altman, Shyamal Anadkat, et al. Gpt-4 technical
560 report. *arXiv preprint arXiv:2303.08774*, 2023.

561 Meta AI. Introducing llama 3.1: Our most capable models to date. [https://ai.meta.com/
562 blog/meta-llama-3-1/](https://ai.meta.com/blog/meta-llama-3-1/), 2024. Accessed: 2024-07-23.

563 Alexander A Alemi, Ian Fischer, Joshua V Dillon, and Kevin Murphy. Deep variational information
564 bottleneck. *arXiv preprint arXiv:1612.00410*, 2016.

565 Amos Azaria and Tom Mitchell. The internal state of an llm knows when it's lying. *arXiv preprint
566 arXiv:2304.13734*, 2023.

567 Gregor Bachmann and Vaishnavh Nagarajan. The pitfalls of next-token prediction. In *International
568 Conference on Machine Learning*, pp. 2296–2318. PMLR, 2024.

569 Jiaqi Bai, Hongcheng Guo, Zhongyuan Peng, Jian Yang, Zhoujun Li, Mohan Li, and Zhihong Tian.
570 Mitigating hallucinations in large vision-language models by adaptively constraining information
571 flow. In *Proceedings of the AAAI Conference on Artificial Intelligence*, volume 39, pp. 23442–
572 23450, 2025.

573 Kevin Black, Michael Janner, Yilun Du, Ilya Kostrikov, and Sergey Levine. Training diffusion
574 models with reinforcement learning. In *The Twelfth International Conference on Learning Rep-
575 resentations*, 2024.

576 Collin Burns, Haotian Ye, Dan Klein, and Jacob Steinhardt. Discovering latent knowledge in lan-
577 guage models without supervision. *arXiv preprint arXiv:2212.03827*, 2022.

578 Chao Chen, Kai Liu, Ze Chen, Yi Gu, Yue Wu, Mingyuan Tao, Zhihang Fu, and Jieping
579 Ye. Inside: Llms' internal states retain the power of hallucination detection. *arXiv preprint
580 arXiv:2402.03744*, 2024a.

581 Zhongzhi Chen, Xingwu Sun, Xianfeng Jiao, Fengzong Lian, Zhanhui Kang, Di Wang, and
582 Chengzhong Xu. Truth forest: Toward multi-scale truthfulness in large language models through
583 intervention without tuning. In *Proceedings of the AAAI Conference on Artificial Intelligence*,
584 volume 38, pp. 20967–20974, 2024b.

585 I Chern, Steffi Chern, Shiqi Chen, Weizhe Yuan, Kehua Feng, Chunting Zhou, Junxian He, Gra-
586 ham Neubig, Pengfei Liu, et al. Factool: Factuality detection in generative ai—a tool augmented
587 framework for multi-task and multi-domain scenarios. *arXiv preprint arXiv:2307.13528*, 2023.

594 Xuefeng Du, Chaowei Xiao, and Sharon Li. Haloscope: Harnessing unlabeled llm generations for
 595 hallucination detection. *Advances in Neural Information Processing Systems*, 37:102948–102972,
 596 2024.

597

598 Lei Huang, Weijiang Yu, Weitao Ma, Weihong Zhong, Zhangyin Feng, Haotian Wang, Qianglong
 599 Chen, Weihua Peng, Xiaocheng Feng, Bing Qin, et al. A survey on hallucination in large language
 600 models: Principles, taxonomy, challenges, and open questions. *ACM Transactions on Information
 601 Systems*, 43(2):1–55, 2025.

602 Eric Jang, Shixiang Gu, and Ben Poole. Categorical reparameterization with gumbel-softmax. *arXiv
 603 preprint arXiv:1611.01144*, 2016.

604

605 Mandar Joshi, Eunsol Choi, Daniel S Weld, and Luke Zettlemoyer. Triviaqa: A large scale distantly
 606 supervised challenge dataset for reading comprehension. *arXiv preprint arXiv:1705.03551*, 2017.

607 Hazel Kim, Adel Bibi, Philip Torr, and Yarin Gal. Detecting llm hallucination through layer-wise
 608 information deficiency: Analysis of unanswerable questions and ambiguous prompts. *arXiv
 609 preprint arXiv:2412.10246*, 2024.

610

611 Jannik Kossen, Jiatong Han, Muhammed Razzak, Lisa Schut, Shreshth Malik, and Yarin Gal.
 612 Semantic entropy probes: Robust and cheap hallucination detection in llms. *arXiv preprint
 613 arXiv:2406.15927*, 2024.

614

615 Lorenz Kuhn, Yarin Gal, and Sebastian Farquhar. Semantic uncertainty: Linguistic invariances for
 616 uncertainty estimation in natural language generation. *arXiv preprint arXiv:2302.09664*, 2023.

617

618 Solomon Kullback and Richard A Leibler. On information and sufficiency. *The annals of mathe-
 619 matical statistics*, 22(1):79–86, 1951.

620

621 Kenneth Li, Oam Patel, Fernanda Viégas, Hanspeter Pfister, and Martin Wattenberg. Inference-time
 622 intervention: Eliciting truthful answers from a language model. *Advances in Neural Information
 623 Processing Systems*, 36:41451–41530, 2023.

624

625 Xiang Li, John Thickstun, Ishaan Gulrajani, Percy S Liang, and Tatsumori B Hashimoto. Diffusion-
 626 lm improves controllable text generation. *Advances in neural information processing systems*, 35:
 627 4328–4343, 2022.

628

629 Zhuowei Li, Haizhou Shi, Yunhe Gao, Di Liu, Zhenting Wang, Yuxiao Chen, Ting Liu, Long Zhao,
 630 Hao Wang, and Dimitris N Metaxas. The hidden life of tokens: Reducing hallucination of large
 631 vision-language models via visual information steering. In *Forty-second International Conference
 632 on Machine Learning*, 2025.

633

634 Stephanie Lin, Jacob Hilton, and Owain Evans. Teaching models to express their uncertainty in
 635 words. *arXiv preprint arXiv:2205.14334*, 2022.

636

637 Zhen Lin, Shubhendu Trivedi, and Jimeng Sun. Generating with confidence: Uncertainty quantifi-
 638 cation for black-box large language models. *arXiv preprint arXiv:2305.19187*, 2023.

639

640 Qiang Liu, Xinlong Chen, Yue Ding, Bowen Song, Weiqiang Wang, Shu Wu, and Liang Wang.
 641 Attention-guided self-reflection for zero-shot hallucination detection in large language models.
 642 *arXiv preprint arXiv:2501.09997*, 2025a.

643

644 Sheng Liu, Haotian Ye, and James Zou. Reducing hallucinations in large vision-language models via
 645 latent space steering. In *The Thirteenth International Conference on Learning Representations*,
 646 2025b.

647

648 Zichuan Liu, Tianchun Wang, Jimeng Shi, Xu Zheng, Zhuomin Chen, Lei Song, Wenqian Dong,
 649 Jayantha Obeysekera, Farhad Shirani, and Dongsheng Luo. Timex++: Learning time-series ex-
 650 planations with information bottleneck. *arXiv preprint arXiv:2405.09308*, 2024.

651

652 Rui Lu, Runzhe Wang, Kaifeng Lyu, Xitai Jiang, Gao Huang, and Mengdi Wang. Towards un-
 653 derstanding text hallucination of diffusion models via local generation bias. In *The Thirteenth
 654 International Conference on Learning Representations*, 2025.

648 Yawei Luo, Ping Liu, Tao Guan, Junqing Yu, and Yi Yang. Significance-aware information bottle-
 649 neck for domain adaptive semantic segmentation. In *Proceedings of the IEEE/CVF international*
 650 *conference on computer vision*, pp. 6778–6787, 2019.

651

652 Mahdi Farrokhi Maleki and Richard Zhao. Procedural content generation in games: A survey with
 653 insights on emerging llm integration. In *Proceedings of the AAAI Conference on Artificial Intel-*
 654 *ligence and Interactive Digital Entertainment*, volume 20, pp. 167–178, 2024.

655

656 Andrey Malinin and Mark Gales. Uncertainty estimation in autoregressive structured prediction.
 657 *arXiv preprint arXiv:2002.07650*, 2020.

658

659 Potsawee Manakul, Adian Liusie, and Mark JF Gales. Selfcheckgpt: Zero-resource black-box hallu-
 660 *cination detection for generative large language models. arXiv preprint arXiv:2303.08896*, 2023.

661

662 Samuel Marks and Max Tegmark. The geometry of truth: Emergent linear structure in large language
 663 model representations of true/false datasets. *arXiv preprint arXiv:2310.06824*, 2023.

664

665 Sewon Min, Kalpesh Krishna, Xinxi Lyu, Mike Lewis, Wen-tau Yih, Pang Wei Koh, Mohit Iyyer,
 666 Luke Zettlemoyer, and Hannaneh Hajishirzi. Factscore: Fine-grained atomic evaluation of factual
 667 precision in long form text generation. *arXiv preprint arXiv:2305.14251*, 2023.

668

669 Fan Nie, Xiaotian Hou, Shuhang Lin, James Zou, Huaxiu Yao, and Linjun Zhang. Facttest: Factu-
 670 *ality testing in large language models with finite-sample and distribution-free guarantees*, 2024.
 671 URL <https://arxiv.org/abs/2411.02603>.

672

673 Shen Nie, Fengqi Zhu, Zebin You, Xiaolu Zhang, Jingyang Ou, Jun Hu, Jun Zhou, Yankai
 674 Lin, Ji-Rong Wen, and Chongxuan Li. Large language diffusion models. *arXiv preprint*
 675 *arXiv:2502.09992*, 2025.

676

677 Hadas Orgad, Michael Toker, Zorik Gekhman, Roi Reichart, Idan Szpektor, Hadas Kotek, and
 678 Yonatan Belinkov. Llms know more than they show: On the intrinsic representation of llm hallu-
 679 *cinations. In The Thirteenth International Conference on Learning Representations*, 2025.

680

681 Seongheon Park, Xuefeng Du, Min-Hsuan Yeh, Haobo Wang, and Yixuan Li. Steer llm latents for
 682 *hallucination detection. arXiv preprint arXiv:2503.01917*, 2025.

683

684 Owen Queen, Tom Hartvigsen, Teddy Koker, Huan He, Theodoros Tsiligkaridis, and Marinka Zit-
 685 *nik. Encoding time-series explanations through self-supervised model behavior consistency. Ad-*
 686 *vances in Neural Information Processing Systems*, 36:32129–32159, 2023.

687

688 Vipula Rawte, Amit Sheth, and Amitava Das. A survey of hallucination in large foundation models.
 689 *arXiv preprint arXiv:2309.05922*, 2023.

690

691 Jie Ren, Jiaming Luo, Yao Zhao, Kundan Krishna, Mohammad Saleh, Balaji Lakshminarayanan,
 692 and Peter J Liu. Out-of-distribution detection and selective generation for conditional language
 693 models. *arXiv preprint arXiv:2209.15558*, 2022.

694

695 Subham Sahoo, Marianne Arriola, Yair Schiff, Aaron Gokaslan, Edgar Marroquin, Justin Chiu,
 696 Alexander Rush, and Volodymyr Kuleshov. Simple and effective masked diffusion language
 697 models. *Advances in Neural Information Processing Systems*, 37:130136–130184, 2024.

698

699 Jiaxin Shi, Kehang Han, Zhe Wang, Arnaud Doucet, and Michalis Titsias. Simplified and general-
 700 *ized masked diffusion for discrete data. Advances in neural information processing systems*, 37:
 701 103131–103167, 2024.

702

703 Weihang Su, Changyue Wang, Qingyao Ai, Yiran Hu, Zijing Wu, Yujia Zhou, and Yiqun Liu. Un-
 704 *supervised real-time hallucination detection based on the internal states of large language models.*
 705 *arXiv preprint arXiv:2403.06448*, 2024.

706

707 Zhongxiang Sun, Xiaoxue Zang, Kai Zheng, Yang Song, Jun Xu, Xiao Zhang, Weijie Yu, and Han
 708 Li. Redep: Detecting hallucination in retrieval-augmented generation via mechanistic inter-
 709 *pretability. arXiv preprint arXiv:2410.11414*, 2024.

702 Alon Talmor, Jonathan Herzig, Nicholas Lourie, and Jonathan Berant. Commonsenseqa: A question
 703 answering challenge targeting commonsense knowledge. *arXiv preprint arXiv:1811.00937*, 2018.
 704

705 Naftali Tishby and Noga Zaslavsky. Deep learning and the information bottleneck principle. In
 706 *2015 ieee information theory workshop (itw)*, pp. 1–5. Ieee, 2015.

707 Naftali Tishby, Fernando C Pereira, and William Bialek. The information bottleneck method. *arXiv
 708 preprint physics/0004057*, 2000.
 709

710 Ashish Vaswani, Noam Shazeer, Niki Parmar, Jakob Uszkoreit, Llion Jones, Aidan N Gomez,
 711 Łukasz Kaiser, and Illia Polosukhin. Attention is all you need. *Advances in neural informa-
 712 tion processing systems*, 30, 2017.

713 Peter West, Ari Holtzman, Jan Buys, and Yejin Choi. Bottlesum: Unsupervised and self-
 714 supervised sentence summarization using the information bottleneck principle. *arXiv preprint
 715 arXiv:1909.07405*, 2019.

716 Miao Xiong, Zhiyuan Hu, Xinyang Lu, Yifei Li, Jie Fu, Junxian He, and Bryan Hooi. Can llms
 717 express their uncertainty? an empirical evaluation of confidence elicitation in llms. *arXiv preprint
 718 arXiv:2306.13063*, 2023.
 719

720 An Yang, Anfeng Li, Baosong Yang, Beichen Zhang, Binyuan Hui, Bo Zheng, Bowen Yu,
 721 Chang Gao, Chengan Huang, Chenxu Lv, et al. Qwen3 technical report. *arXiv preprint
 722 arXiv:2505.09388*, 2025a.

723 Ling Yang, Zhilong Zhang, Yang Song, Shenda Hong, Runsheng Xu, Yue Zhao, Wentao Zhang,
 724 Bin Cui, and Ming-Hsuan Yang. Diffusion models: A comprehensive survey of methods and
 725 applications. *ACM computing surveys*, 56(4):1–39, 2023.
 726

727 Ling Yang, Ye Tian, Bowen Li, Xinchen Zhang, Ke Shen, Yunhai Tong, and Mengdi Wang. Mmada:
 728 Multimodal large diffusion language models. *arXiv preprint arXiv:2505.15809*, 2025b.

729 Zhilin Yang, Peng Qi, Saizheng Zhang, Yoshua Bengio, William W Cohen, Ruslan Salakhutdinov,
 730 and Christopher D Manning. Hotpotqa: A dataset for diverse, explainable multi-hop question
 731 answering. *arXiv preprint arXiv:1809.09600*, 2018.
 732

733 Shunyu Yao, Jeffrey Zhao, Dian Yu, Nan Du, Izhak Shafran, Karthik Narasimhan, and Yuan Cao.
 734 React: Synergizing reasoning and acting in language models. In *International Conference on
 735 Learning Representations (ICLR)*, 2023.

736 Jiacheng Ye, Zhihui Xie, Lin Zheng, Jiahui Gao, Zirui Wu, Xin Jiang, Zhenguo Li, and Lingpeng
 737 Kong. Dream 7b: Diffusion large language models. *arXiv preprint arXiv:2508.15487*, 2025.
 738

739 Yue Zhang, Yafu Li, Leyang Cui, Deng Cai, Lemao Liu, Tingchen Fu, Xinting Huang, Enbo Zhao,
 740 Yu Zhang, Yulong Chen, et al. Siren’s song in the ai ocean: A survey on hallucination in large
 741 language models. *Computational Linguistics*, pp. 1–46, 2025.

742 Siyan Zhao, Devaansh Gupta, Qinqing Zheng, and Aditya Grover. d1: Scaling reasoning in diffusion
 743 large language models via reinforcement learning. *arXiv preprint arXiv:2504.12216*, 2025.
 744

745 Kun Zhu, Xiaocheng Feng, Xiyuan Du, Yuxuan Gu, Weijiang Yu, Haotian Wang, Qianglong Chen,
 746 Zheng Chu, Jingchang Chen, and Bing Qin. An information bottleneck perspective for effective
 747 noise filtering on retrieval-augmented generation. *arXiv preprint arXiv:2406.01549*, 2024.
 748

749

750

751

752

753

754

755

756

A USAGE OF LLMs

758 For transparency, we report our use of LLMs. We employed OpenAI ChatGPT solely to assist
 759 with language polishing, copy editing, and improving exposition in terms of grammar, phrasing,
 760 and organization. In addition, we used Qwen-8B as an external judge for hallucination detection
 761 in open-domain QA, but its outputs were carefully checked by the authors. None of these LLMs
 762 was used to (i) generate scientific hypotheses or claims; (ii) design experiments; (iii) perform data
 763 collection, processing, or analysis; (iv) compute metrics or produce numerical results; or (v) create
 764 figures. All substantive content, experimental procedures, and numerical results were produced by
 765 the authors. The corresponding author assumes full responsibility for ensuring the accuracy and
 766 integrity of the paper.

767

B DETAILED RELATED WORK

770 **Baseline Methods.** We compare our method against seven baselines spanning two categories pro-
 771 posed in Section 4.

772 (1) *Output-based methods*: These methods operate only on the generated text, detecting hallucina-
 773 tions by analyzing uncertainty or surface similarity.

775 - **Perplexity** (Ren et al., 2022): computes the negative log-likelihood of the generated sequence
 776 under the base model. Higher perplexity indicates that the model assigns low probability to its own
 777 output, suggesting potential hallucination.

778 - **Length-Normalized Entropy (LN-Entropy)** (Malinin & Gales, 2020): measures the token-level
 779 predictive entropy of the output distribution, normalized by sequence length, so that generations
 780 with unusually high average uncertainty are flagged as hallucinations.

781 - **Semantic Entropy** (Kuhn et al., 2023): measures consistency of multiple generations by parti-
 782 tioning them into semantic classes and computing the entropy of this class distribution. A higher
 783 semantic entropy indicates greater uncertainty, which is taken as a signal of hallucination.

785 - **Lexical Similarity** (Lin et al., 2023): assesses consistency of multiple generations using lexical
 786 overlap metrics. Low overlap suggests divergence from supporting evidence, which is interpreted as
 787 hallucination.

788 (2) *Latent-based methods*. These approaches exploit hidden states or latent directions of LLMs,
 789 probing truthfulness signals directly from internal representations.

790 - **EigenScore** (Chen et al., 2024a): proposed in INSIDE (ICLR 2024), it measures response consis-
 791 tency via the log-determinant of the covariance matrix of their latent embeddings.

792 - **Contrast-Consistent Search (CCS)** (Burns et al., 2022): queries the model with contrastive
 793 prompts (e.g., factual vs. hallucinated) and trains a MLP to evaluate consistency of latent repre-
 794 sentations. Inconsistent activations are interpreted as evidence of hallucination.

796 - **Truthfulness Separator Vector (TSV)** (Park et al., 2025): Trains a steering vector that separates
 797 truthful from hallucinated generations in latent space, and then classifies new samples by projecting
 798 onto the learned centroids.

799 **Other potential baselines.** Several alternative baselines for hallucination detection exist, however
 800 they are challenging to implement in comparison to our proposed method. One major category,
 801 highlighted in Huang et al. (2025), is fact-checking external retrieval methods, including: **FactScore**
 802 (Min et al., 2023), which decomposes long-form text into fact chunks and computes the proportion of
 803 chunks verified by an external knowledge base. And, **Factool** (Chern et al., 2023), a tool-augmented
 804 method enabling LLMs to detect factual hallucinations using external resources. These approaches
 805 rely on additional knowledge sources (e.g., Wikipedia or local databases), which conflicts with our
 806 core objective of detecting hallucinations *without external verification*.

807 Other recent hallucination methods include:

809 • **ReDeEP** (Sun et al., 2024), a method specifically designed for Retrieval-Augmented Generation
 (RAG). It disentangles retrieved evidence from the LLM’s parametric knowledge, then measures

810 the alignment between the two. While effective in RAG settings, it is task-specific: in our
 811 internal-signal-based experiments, there is no retrieved context to disentangle, so ReDeEP is not
 812 applicable.
 813
 814

815 • **FactTest** (Nie et al., 2024), which formulates hallucination detection as a distribution-free hy-
 816 pothesis testing problem. It controls Type I error by introducing an abstention mechanism, re-
 817 quiring a held-out calibration dataset and repeated testing procedures. Although statistically
 818 elegant, this framework is fundamentally different from our design goal: we aim for lightweight
 819 detection relying purely on model-internal dynamics, without the need for extra calibration data
 820 or abstention strategies.
 821
 822

823 • **AGSER** (Liu et al., 2025a), which leverages attention-guided self-reflection. It analyzes self-
 824 attention maps, distinguishes “attentive” vs. “non-attentive” tokens, and trains a secondary clas-
 825 sifier on the distribution of attention patterns to identify hallucinations. This approach depends
 826 on full access to intermediate attention weights and assumes an autoregressive token-to-token at-
 827 tention structure. However, D-LLMs adopt denoising architectures where attention is not aligned
 828 with autoregressive decoding, making AGSER difficult to adapt. Additionally, extracting and
 829 processing large attention tensors incurs substantial computational overhead, which goes against
 830 our efficiency-oriented design.
 831
 832

832 Overall, while these methods are valuable in their respective contexts, their reliance on external re-
 833 sources, additional datasets, or architectural assumptions makes them unsuitable as direct baselines
 834 for our study. For this reason, we do not include them in the main comparison and instead discuss
 835 them here for completeness.
 836
 837
 838

839 C ALGORITHMS

840
 841
 842 We provide the pseudo-code of our method in Algorithm 1.
 843
 844
 845

846 D MORE ON EQ 4 AND EQ 5

850 D.1 EQ 4

$$\begin{aligned}
 I(Y; A_{\text{sub}}) &= \int P(y, A_{\text{sub}}) \log \frac{P(y | A_{\text{sub}})}{P(y)} dy dA_{\text{sub}} \\
 &= \int P(y, A_{\text{sub}}) \log P(y | A_{\text{sub}}) dy dA_{\text{sub}} - \int P(y, A_{\text{sub}}) \log P(y) dy dA_{\text{sub}} \\
 &= \int P(y, A_{\text{sub}}) \log P(y | A_{\text{sub}}) dy dA_{\text{sub}} + H(Y) \\
 &\geq \int P(y, A_{\text{sub}}) \log q_{\theta}(y | A_{\text{sub}}) dy dA_{\text{sub}} \\
 &= \mathbb{E}_{Y, A_{\text{sub}}} [\log q_{\theta}(Y | A_{\text{sub}})] := -\mathcal{L}_{cls}
 \end{aligned}$$

864 **Algorithm 1** Overall training framework for TRACEDET

865 1: **Parameters:** batch size B , prior masking ratio r , extraction weight β
 866 2: **Inputs:** Entropy sequence $A \in \mathbb{R}^{T \times B \times D}$
 867 3: **Initialize:** Transformer encoder with random weights
 868 4: **Input encoding:**
 869 5: Project A using MLP-based positional encoder
 870 6: Concatenate sinusoidal time embeddings of dimension d_{pe}
 871 7: Apply Transformer encoder to obtain contextual embeddings $\text{emb} \in \mathbb{R}^{T \times B \times d_{\text{ff}}}$
 872 8: **Sub-instance extraction:**
 873 9: **for** $t = 1$ to T **do**
 874 10: **for** $b = 1$ to B **do**
 875 11: Compute cross attention: $att = \text{attn}(\text{emb}, A)$
 876 12: Apply linear layer and softmax over time steps: $\hat{m}_{t,b} = \text{softmax}(\text{Linear}(att))$
 877 13: **end for**
 878 14: **end for**
 879 15: Apply masking: $A_{\text{sub}} = M \odot A$
 880 16: **Sub-instance classification:**
 881 17: **for** $b = 1$ to B **do**
 882 18: Aggregate temporally: $A'_{\text{sub}} = \text{Mean}(A_{\text{sub}, \cdot, b, \cdot})$
 883 19: Compute hallucination probability: $\hat{y}_b = \text{ReLU-MLP}(A'_{\text{sub}})$
 884 20: **end for**
 885 21: **Training objective:**
 886 22: Classification loss: $\mathcal{L}_{\text{cls}} = \text{BCE}(\hat{y}_b, y_b)$
 887 23: Extraction regularizer:
 888 24: Total loss: $\mathcal{L} = \mathcal{L}_{\text{cls}} + \beta \mathcal{L}_{\text{ext}}$
 889 25: Backpropagate and update parameters

893
 894
 895 **D.2 EQ 5**

896
 897
 898
$$I(A; A_{\text{sub}}) = \mathbb{E}_{A, A_{\text{sub}}} \left[\log \frac{P(A_{\text{sub}} | A)}{P(A_{\text{sub}})} \right]$$

 899
 900
$$= \mathbb{E}_{A, A_{\text{sub}}} \left[\log \frac{P(A_{\text{sub}} | A)Q(A_{\text{sub}})}{P(A_{\text{sub}})Q(A_{\text{sub}})} \right]$$

 901
 902
$$= \mathbb{E}_{A, A_{\text{sub}}} \left[\log \frac{P(A_{\text{sub}} | A)}{Q(A_{\text{sub}})} \right] - \mathbb{E}_{A, A_{\text{sub}}} \left[\log \frac{Q(A_{\text{sub}})}{P(A_{\text{sub}})} \right]$$

 903
 904
$$= \mathbb{E}_{A, A_{\text{sub}}} \left[\log \frac{P(A_{\text{sub}} | A)}{Q(A_{\text{sub}})} \right] - D_{\text{KL}}(P(A_{\text{sub}}) \| Q(A_{\text{sub}}))$$

 905
 906
 907
 908
$$\leq \mathbb{E}_A \left[D_{\text{KL}}(P(A_{\text{sub}} | A) \| Q(A_{\text{sub}})) \right]$$

911
 912 **D.3 PROOF OF RELAXATION**

913
 914
 915
 916 **KL decomposition under independent Bernoulli factors.** Under the independence assumption,
 917 both the true posterior $P(A_{\text{sub}} | A)$ and the variational prior $Q(A_{\text{sub}})$ factorize into products of
 Bernoulli distributions. In this case, the KL divergence decomposes into a sum of element-wise

918 Bernoulli KL terms:

919
920
$$D_{\text{KL}}(P(A_{\text{sub}} \mid A) \parallel Q(A_{\text{sub}})) = \sum_i D_{\text{KL}}(\text{Bern}(p_{a_i}) \parallel \text{Bern}(\tau)).$$

921

922
923 **KL divergence between two Bernoulli variables.** For a single Bernoulli distribution, the KL
924 divergence has the following closed form:

925
926
$$D_{\text{KL}}(\text{Bern}(p) \parallel \text{Bern}(\tau)) = p \log \frac{p}{\tau} + (1-p) \log \frac{1-p}{1-\tau}.$$

927

928

E EXPERIMENT SETTINGS

929930 All experiments were conducted on NVIDIA A40 GPUs. Hyperparameter settings are shown in
931 Tabel 5.
932933 Table 5: Hyperparameter search space for TRACEDET. *Notation:* \dagger log-spaced; \ddagger linearly spaced. $*$
934 only applies to LLaDA.

Parameter	Range	Grid size
Learning rate (<i>lr</i>)	$[10^{-5}, 10^{-3}]^\dagger$	8
Batch size (<i>batch_size</i>)	{8, 64}	2
Dropout rate (<i>dropout_rate</i>)	$[0.0, 0.4]^\ddagger$	5
Number of layers (<i>nlayers</i>)	{2, 3, 4}	3
β	$[0, 2]^\ddagger$	6
τ	$[0.1, 0.4]^\ddagger$	4
cfg*	{0, 1}	2

944
945

F CASE STUDY

946947

F.1 INTERLEAVING HALLUCINATION

948949

Retained Steps

950
951

```
<Question>Professor A. Selvanathan is a professor at a university that is public or pri-  
952 vate?</Question>  
953 <Golden label>public</Golden label>  
954 The following are TraceDet extracted steps  
955 <step><answer>public</answer></step>  
956 <step><answer>Public</answer></step>  
957 <step><answer>private</answer></step>  
958 <step><answer>private</answer></step>  
959 <Output><answer>private</answer></Output>
```

960

Retained Step

961962

```
<Question>Friggatriskaidekaphobia (or triskaidekaphobia or paraskevidekatriaphobia) is the fear of  
963 what?</Question>  
964 <Golden label>Friday the 13</Golden label>  
965 The following are TraceDet extracted steps  
966 <step><answer> Friggriskagk anythingobia (or frost excessive or kevide atr13 is the fear of numbers.</answer></step>  
967 <step><answer> Friggriskak thingsobia (oriska k refrigeration oranswerkevide atriobia) is the fear of ice. </answer></step>  
968 <step><answer>Friggatriskakobia (oriskak orkevideatri) is fear of freezing.</answer></step>  
969 <Output><answer>Friggatriskaidekaphobia (or triskaidekaphobia or paraskevidekatriaphobia) is  
970 the fear of numbers.</answer></Output>
```

972

973

Retained Steps

<Question>On which of the hills of ancient Rome were the main residences of the Caesars?</Question>
<Golden label>Palatine</Golden label>
The following are TraceDet extracted steps
<step><answer>Palatine</answer></step>
<step><answer>Palatine</answer></step>
<step><answer>Pal Hill Hill</answer></step>
<step><answer>Palat Hill</answer></step>
<Output><answer>Palat Hill</answer></Output>

982

983

984

Retained Steps

<Question>What NFL Premier Intermediate League team did Sean Connor play for?</Question>
<Golden label>Distillery</Golden label>
The following are TraceDet extracted steps
<step><answer>Distillery F.C</answer></step>
<step><answer>Newis Distillery F.C</answer></step>
<step><answer>Newington Youth.C.C.</answer></step>
<step><answer>Newington Youth F.C.</answer></step>
<Output><answer>Newington Youth F.C.</answer></Output>

992

993

994

F.2 INCONSISTENT GUESSES

996

Retained Step

101

1012

Retained Step

<Question>Which Canadian born actress was the star in the movie Barb Wire?</Question>

<Golden label>Pamela Anderson</Golden label>

The following are TraceDet extracted steps

Canadian</answer>”, </step>
<step>“<answer>Kirstodie Therellar 55106069</answer>”, anisotropicwald Kirst Kirst
Kirstaghanaghan Barb</answer>”, </step>

<Output><answer>Kirstie Alley</answer></Output>

1026
1027

F.3 PERSISTENT ERROR

1028
1029

Retained Step

1030
1031

<Question>In the Shakespeare play The Tempest, Prospero is the overthrown Duke of where?</Question>
 <Golden label>The weather in Milan</Golden label>
 The following are TraceDet extracted steps
 <step>”InIn Shakespeare play Temp Temp Temp Prosper Prosper Prosper Prosper Prosper Prosper
 Prosperrownrown Duke Duke Prosperiel. Prosper;answer;In Prosper Shakespeare playThe Tempest,
 Prospero Prosper Prosper overthrown Duke of ‘Ariiel’,</step>
 <step>” In the Shakespeare play,o is thethrown Duke of ‘ overthrown Duke of 2018ieliel. ;answer; In
 Shakespeare play Theest,o is the overrown Duke of ‘Ariiel’, </step>
 <step>”In Shakespeare play The, is thethrown Duke of ‘Ariiel’. In the Shakespeare play Theest,
 Prospero is the overthrown Duke of ‘Ariiel’., </step>
 <step>”In the Shakespeare play The Tempest, Prospero is the overthrown Duke of ‘Ariiel’”, </step>
 <Output>”In the Shakespeare play The Tempest, Prospero is the overthrown Duke of ‘Ariiel’”</Output>

1042
1043

G ADDITIONAL QUANTITATIVE RESULTS

1044

Table 6: TPR@FPR=0.1 (%) comparison between TraceDet and baseline methods. The highest score is **bolded**.

1045

1046

1047

1048

Method	TriviaQA		HotpotQA		CommonsenseQA	
	128	64	128	64	128	64
Lexical Similarity	14.5	15.6	19.8	19.3	0.0	0.0
EigenScore	23.9	29.6	23.5	24.1	40.2	26.8
CCS	9.0	26.9	11.8	10.3	14.2	19.5
TSV	23.5	26.8	14.1	16.1	23.6	14.6
TraceDet	41.4	59.6	19.3	39.1	61.5	61.6

1049

1050
1051

Table 7: Comparison of average epoch training time across TraceDet and training-based baseline methods on TriviaQA using 1700 training samples.

1052

1053

1054

1055

Method	Training Time (s)
CCS	3.64
TSV	19.2
TraceDet	2.25

1056
1057
1058

H TRACEDET IMPLEMENTATION DETAILS

1059

- **Sub-instance extractor.** Given the entropy sequence $A \in \mathbb{R}^{T \times B \times D}$, we first concatenate it with sinusoidal time embeddings and encode the result using a lightweight Transformer (2–5 layers, 1 head, feedforward dimension 8), producing contextual embeddings emb . The extractor then generates a probabilistic mask $\hat{M} \in (0, 1)^{T \times B}$, where each entry is computed as

1060
1061
1062
1063

$$\hat{m}_{t,b} = \text{Linear}(\text{attn}(\text{emb}, A)),$$

1064
1065
1066
1067

and attn denotes a cross-attention module that uses emb as the query and a learned projection of A as the key/value.

1068
1069
1070
1071
1072
1073
1074
1075
1076
1077
1078
1079

To obtain a binary temporal mask $M \in \{0, 1\}^{T \times B}$, we apply a small Transformer encoder (1 layer, 1 head, feedforward dimension 8) to the concatenation of A and emb , followed by a linear layer and a sampling step. The mask is applied element-wise to A to obtain $A_{\text{sub}} = M \odot A \in \mathbb{R}^{T \times B \times D}$. Since the sampling operation is non-differentiable, we employ the Gumbel–Softmax relaxation to enable gradient-based optimization.

1080
1081 • **Sub-instance predictor.** The masked trajectory A_{sub} is temporally aggregated and passed to the
1082 predictor f_{ϕ} , which outputs a hallucination probability for each instance:
1083

$$f_{\phi}(A_{\text{sub}}) \in [0, 1], \quad b = 1, \dots, B.$$

1084 In practice, f_{ϕ} consists of a temporal aggregation module followed by a two-layer MLP.
1085

1086
1087
1088
1089
1090
1091
1092
1093
1094
1095
1096
1097
1098
1099
1100
1101
1102
1103
1104
1105
1106
1107
1108
1109
1110
1111
1112
1113
1114
1115
1116
1117
1118
1119
1120
1121
1122
1123
1124
1125
1126
1127
1128
1129
1130
1131
1132
1133